SHAKE THE FUTURE.

Rapport du Comité de Suivi Individuel

Young Jun Kim[1,2], David Le Touzé[1]

(1) Ecole Centrale de Nantes, France, (2) Bureau Veritas, France

09th / 10 / 2019

General information

- **Affiliation**

  School : École Centrale de Nantes (ECN)
  Lab : LHEEA
  Team : H2I (Hydrodynamique, Interfaces et Interactions)

- **Date of admission**

  01/01/2018 (1 year 10 months)

- **Financement**

  CIFRE contract from Bureau Veritas (BV) and ECN

- **Encadrants de thèse**

  David Le Touzé (Directeur)
  Benjamin Bouscasse (Co-encadrant)

Objective

Numerical improvement and **validation** of a naval hydrodynamics CFD solver in view of performing **fast and accurate** simulation of complex **ship-wave interaction**.

Numerical Improvement

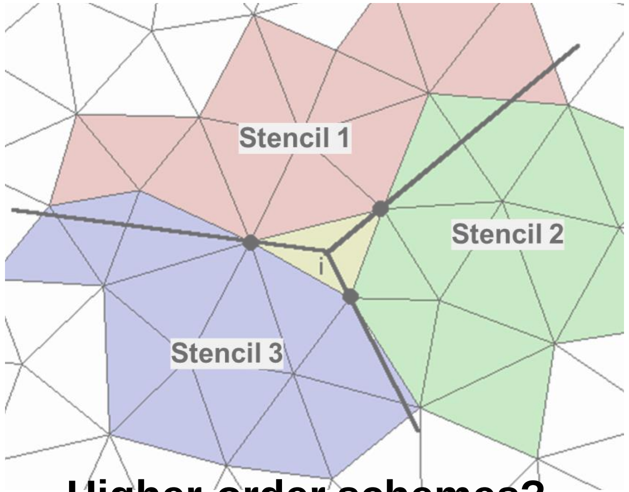

Higher-order schemes?

Efficiency

$$\text{Efficiency} = \frac{\mathit{Accuracy}}{\mathit{Computational\ cost}}$$

Naval applications

One of Petrobras' FPSOs in Brazil; Source: Petrobras

What makes the problem complicated?

Two-phase incompressible viscous (Newtonian) flow solver.

There are many important issues.

The most critical issue is interface (discontinuity).

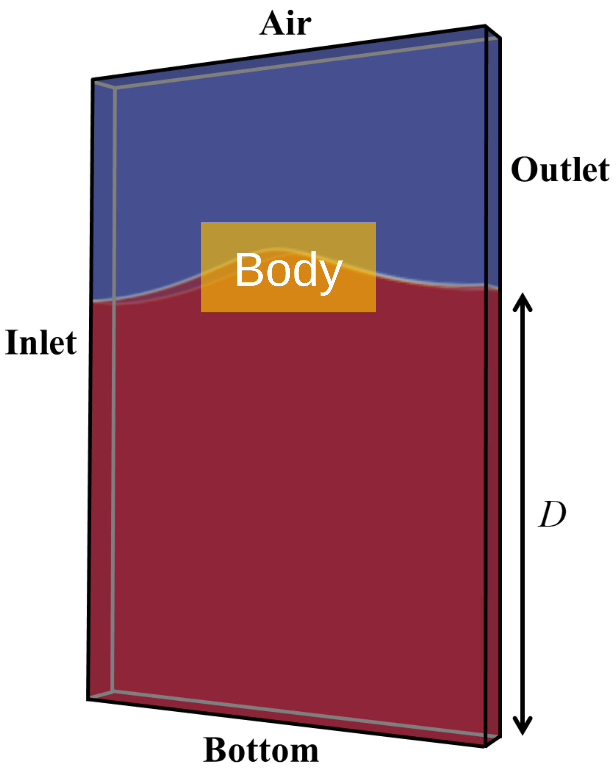

Governing equations

$$\frac{\partial \alpha}{\partial t} + \nabla \cdot (\boldsymbol{u}\alpha) + \nabla \cdot (\boldsymbol{u}_r \alpha (1-\alpha)) = 0$$

$$\frac{\partial (\rho \boldsymbol{u})}{\partial t} + \nabla \cdot (\rho \boldsymbol{u}\boldsymbol{u}) - \nabla \cdot (\mu (\nabla \boldsymbol{u})) - \nabla \boldsymbol{u} \cdot \nabla \mu = \nabla p_d - (\boldsymbol{g} \cdot \boldsymbol{x}) \nabla \rho$$

VOF, density, mass flux, dynamic pressure, viscosity

Preliminary study: Interface treatment

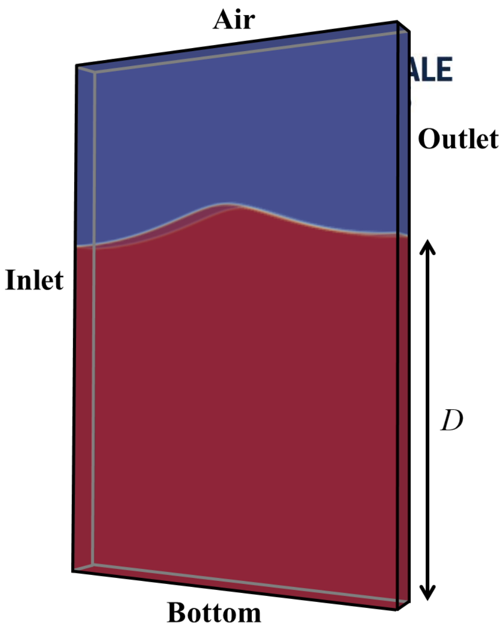

The interface treatment schemes

- Interface capturing scheme: How to define(capture) the free surface.
- Interface advection scheme: How to move interface in time.
- Interface boundary condition: How to define the physical properties at the interface.

Periodic wave propagation test

The interface capturing scheme is VOF.

Interface boundary conditions	Interface advection
Averaged Two-Phase Model	Compressive VOF+MULES
Averaged Two-Phase Model	IsoAdvector
GFM (Ghost Fluid Method)	Compressive VOF+MULES
GFM (Ghost Fluid Method)	IsoAdvector

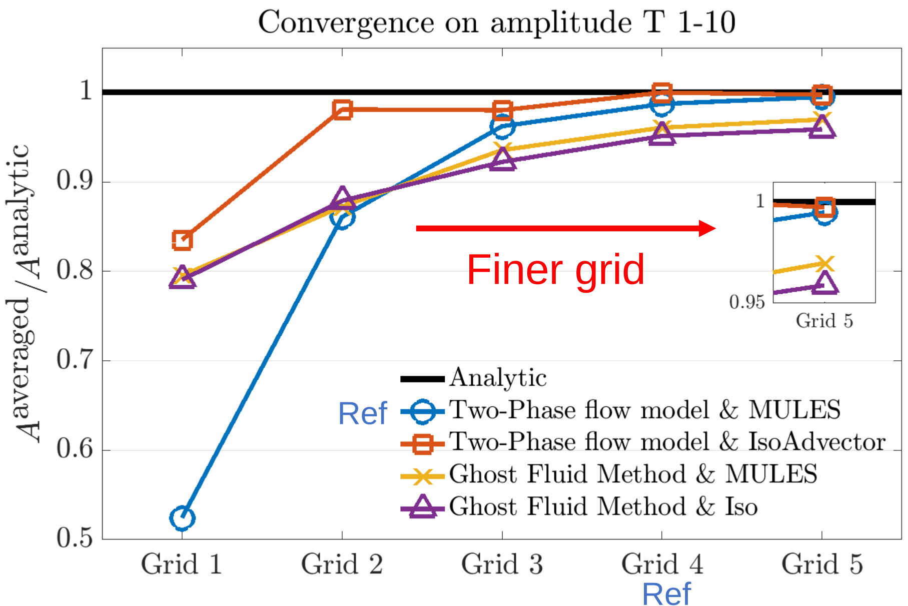

Preliminary study: Waves

Wave generation and absorption.

$$\chi = (1 - w)\chi + w\chi^{Target}$$

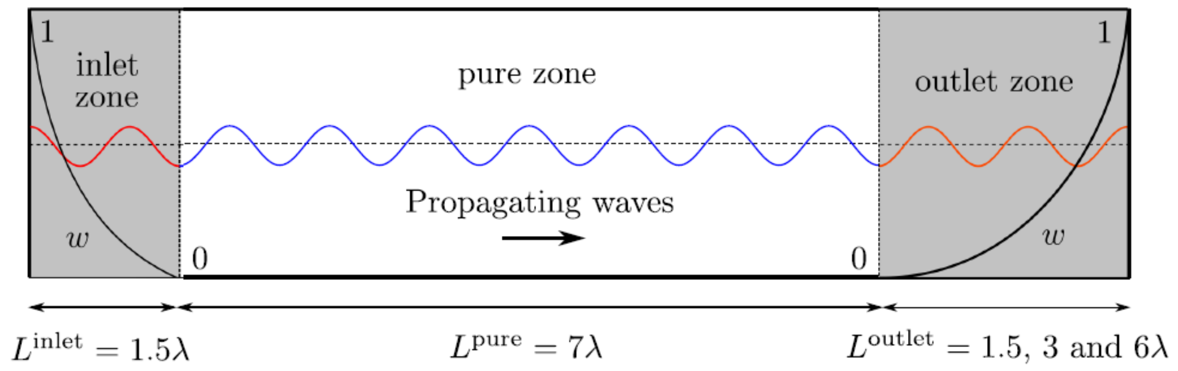

Figure 1.1. Schematic view of the NWT for a parametric study on the relaxation schemes.

Explicit Relaxation method is used to generate wave.

Various outlet conditions are studied

Increased viscosity & artificial damping source

$$\frac{\partial(\rho \boldsymbol{u})}{\partial t} + \nabla\cdot(\rho \boldsymbol{uu}) - \nabla\cdot\left(\left(\mu + \mu_{add}\right)(\nabla \boldsymbol{u})\right) - \nabla \boldsymbol{u}\cdot\nabla\mu = \nabla p_d - (\boldsymbol{g}\cdot\boldsymbol{x})\nabla\rho + \boldsymbol{S}$$

$$\boldsymbol{S} = \left(0, 0, \rho\left(C_1 + C_2 u_z\right) w u_z\right)$$

Relaxation to incident wave & no wave (calm water).

Mesh streatched outlet

Preliminary study: Waves

Wave generation and absorption.

If the condition of outlet is different to the incoming wave, it makes wave reflection and phase shift.

Indicent wave outlet condition gives most stable and precise wave propagation.

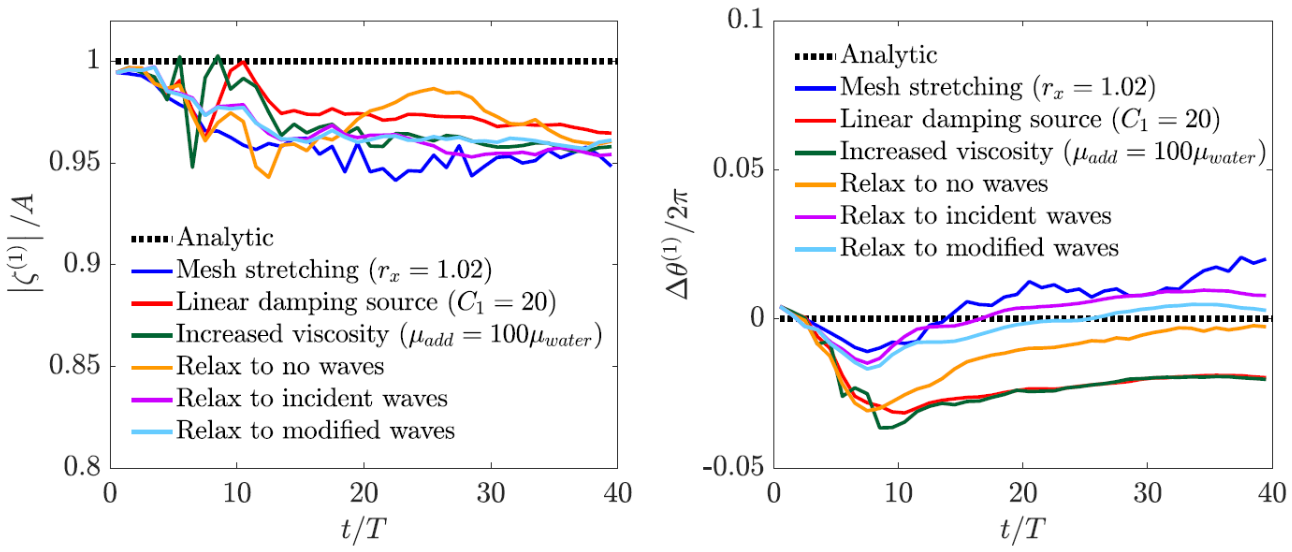

(a) Amplitude (b) Phase differences

Figure 2.1. The first-order harmonic amplitudes and phase differences with respect to different outlet.

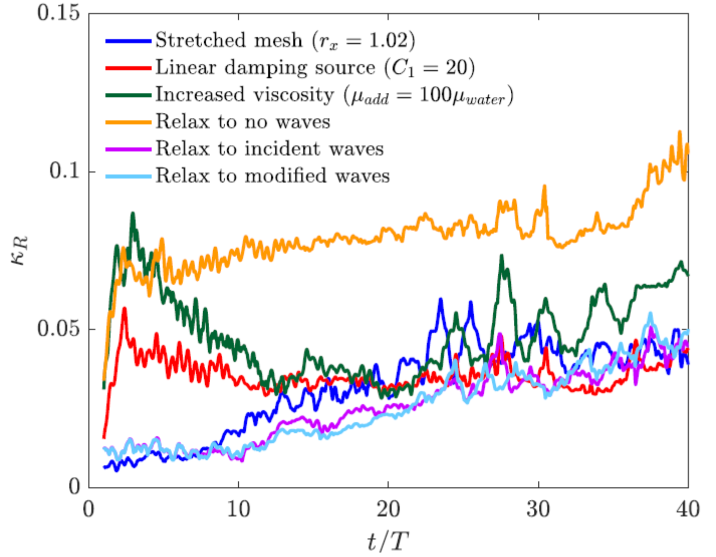

Figure 2.2. Evolution of reflection coefficients for different outlets.

Numerical Improvement Higher-order schemes

Higher-order scheme.

The higher-order schemes are believed to have the advectage on high-order accuracy

Spatial scheme

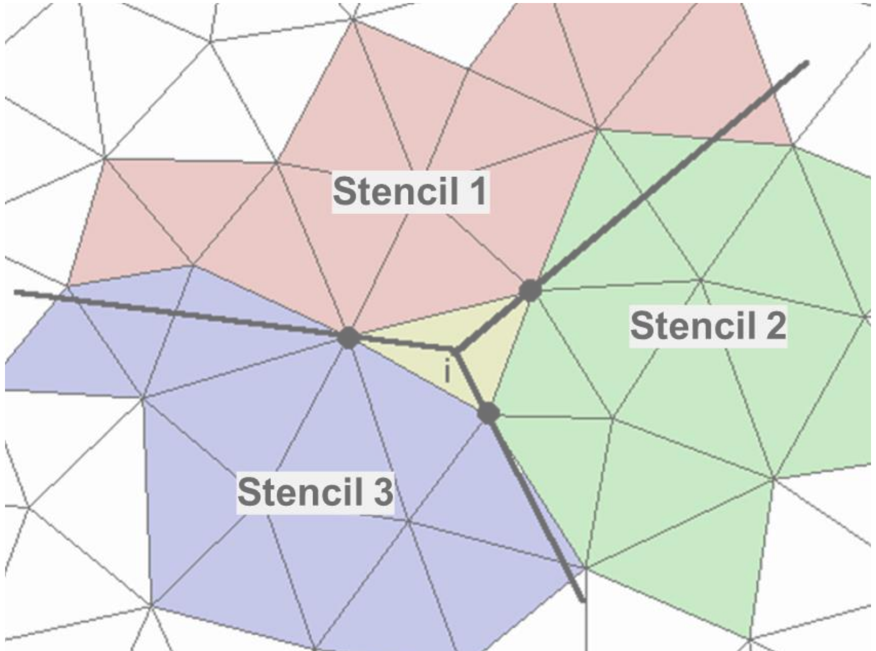

Algorithms and its applications are complicated.

Temporal scheme

$$\frac{dy}{dt} = f(t, y)$$

Consider an ODE

$$\boxed{y^{n+1} = y^n + hf\left(t^{n+1}, y^{n+1}\right)}$$

Implicit Euler

$$\boxed{y^{n+1} = y^n + C_{CN}hf\left(t^{n+1}, y^{n+1}\right) + \left(1 - C_{CN}\right)hf\left(t^n, y^n\right)}$$

Crank Nicolson

$$C\frac{V}{h}\alpha^{t+h} + F(\phi, \alpha)^{t+h} = C_o\frac{V_o}{h}\alpha^t - C_{oo}\frac{V_{oo}}{h}\alpha^{t-h}$$

$$C = 1 + \frac{h}{h + h_o} \qquad C_o = C + C_{oo} \qquad C_o = \frac{h^2}{h_o\left(h + h_o\right)}$$

Second order Backward difference
(Second order Backward differentiation formula (BDF2))

Other ODE Solvers:
Runge Kutta, El...

The temporal schemes are studied first, beacuse it is more simple.

Higher-order temporal schemes

Diagonally Implicit Runge-Kutta (DIRK) method

$$\dot{y} = f(t, y(t)) \tag{1}$$

$$y(t^{(n,i)}) = y^{(i)} = y^{(n)} + \underbrace{h\boxed{a_{ii}}f(t^{(n,i)}, y(t^{(n,i)}))}_{\text{Diagonally implicit}} + \overbrace{h\sum_{j=1}^{i-1} a_{ij} f(t^{(n,j)}, y(t^{(n,j)}))}^{\text{Explicit}} \tag{2}$$

$$t^{(n,i)} = t^{(n)} + h\boxed{\tau_i}$$

$$y^{(n+1)} = y^{(n)} + h\sum_{j=1}^{s} \boxed{b_j} f(t^{(n,j)}, y(t^{(n,j)})) \tag{3}$$

$$\begin{array}{c|cccc} \tau_1 & a_{11} & 0 & 0 & 0 \\ \tau_2 & a_{21} & a_{22} & 0 & 0 \\ \tau_3 & a_{31} & a_{32} & a_{33} & 0 \\ \tau_4 & a_{41} & a_{42} & a_{43} & a_{44} \\ \hline & b_1 & b_2 & b_3 & b_4 \end{array}$$

Butcher matrix

Only SA DIRKs are used.

Singly Diagonally IRK

$$\begin{array}{c|cccc} \tau_1 & \gamma & 0 & 0 & 0 \\ \tau_2 & a_{21} & \gamma & 0 & 0 \\ \tau_3 & a_{31} & a_{32} & \gamma & 0 \\ \tau_4 & a_{41} & a_{42} & a_{43} & \gamma \\ \hline & b_1 & b_2 & b_3 & b_4 \end{array}$$

SDIRK Stiffly accurate

$$\begin{array}{c|cccc} \tau_1 & \gamma & 0 & 0 & 0 \\ \tau_2 & a_{21} & \gamma & 0 & 0 \\ \tau_3 & a_{31} & a_{32} & \gamma & 0 \\ 1 & a_{41} & a_{42} & a_{43} & \gamma \\ \hline & a_{41} & a_{42} & a_{43} & \gamma \end{array}$$

$$\begin{array}{c|cccc} 0 & 0 & 0 & 0 & 0 \\ \tau_2 & a_{21} & \gamma & 0 & 0 \\ \tau_3 & a_{31} & a_{32} & \gamma & 0 \\ \tau_4 & a_{41} & a_{42} & a_{43} & \gamma \\ \hline & b_1 & b_2 & b_3 & b_4 \end{array}$$

Explicit first SDIRK

$$\begin{array}{c|cccc} 0 & 0 & 0 & 0 & 0 \\ \tau_2 & a_{21} & \gamma & 0 & 0 \\ \tau_3 & a_{31} & a_{32} & \gamma & 0 \\ 1 & a_{41} & a_{42} & a_{43} & \gamma \\ \hline & a_{41} & a_{42} & a_{43} & \gamma \end{array}$$

ESDIRK SA

Fig. 1. Four-stage SDIRK, SDIRK_SA, ESDIRK and ESDIRK_SA [14]

Higher-order temporal schemes

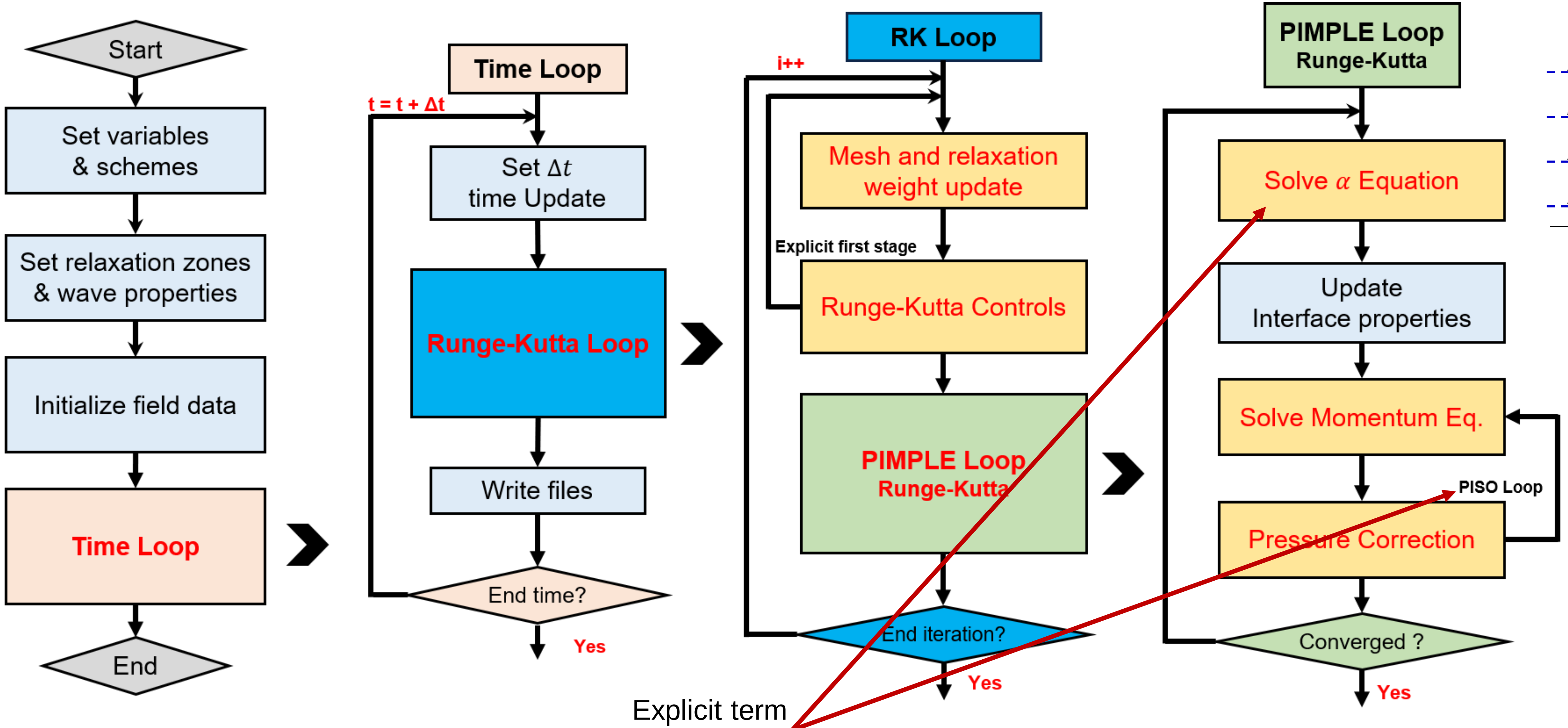

$$
\begin{array}{c|cccc}
\tau_1 & a_{11} & 0 & 0 & 0 \\
\tau_2 & a_{21} & a_{22} & 0 & 0 \\
\tau_3 & a_{31} & a_{32} & a_{33} & 0 \\
\tau_4 & a_{41} & a_{42} & a_{43} & a_{44} \\
\hline
 & b_1 & b_2 & b_3 & b_4
\end{array}
$$

$$y(t^{(n,i)}) = y^{(i)} = y^{(n)} + h a_{ii} f(t^{(n,i)}, y(t^{(n,i)})) + \boxed{h \sum_{j=1}^{i-1} a_{ij} f(t^{(n,j)}, y(t^{(n,j)}))} \quad (2)$$

$$t^{(n,i)} = t^{(n)} + h\tau_i$$

Previous RK iteration data must be used.
Thus, each governing equations must change.

Higher-order temporal schemes

Table 2
Names and the properties of solvers

Code name	Identification name	Order	Implicit stage
Euler	Implicit Euler	1	1
OFCN	OpenFOAM CN	2	1
RKCN	ESDIRK[2](2)_SA	2	1
RK221	SDIRK[2](2)_S	2	2
RK331	SDIRK[3](3)_SA	3	3
RK334	ESDIRK[3](3)_SA	3	2
RK431	ESDIRK[3](4)_SA	$\boxed{3}$	3

RKCN

$$\begin{array}{c|cc} 0 & 0 & 0 \\ 1 & 0.5 & 0.5 \\ \hline & 0.5 & 0.5 \end{array}$$

RK221

$$\begin{array}{c|cc} \gamma & \gamma & 0 \\ 1 & 1-\gamma & \gamma \\ \hline & 1-\gamma & \gamma \end{array}$$

$$\gamma = (2-\sqrt{2})/2$$

RK331

$$\begin{array}{c|ccc} \gamma & \gamma & 0 & 0 \\ \frac{(1+\gamma)}{2} & \frac{(1+\gamma)}{2}-\gamma & \gamma & 0 \\ 1 & -\frac{(6\gamma^2-16\gamma+1)}{4} & \frac{(6\gamma^2-20\gamma+5)}{4} & \gamma \\ \hline & -\frac{(6\gamma^2-16\gamma+1)}{4} & \frac{(6\gamma^2-20\gamma+5)}{4} & \gamma \end{array}$$

$$\gamma = 0.4358665215084589994160194 5.$$

RK431

$$\begin{array}{c|cccc} 0 & 0 & 0 & 0 & 0 \\ 2\gamma & \gamma & \gamma & 0 & 0 \\ c_3 & (c_3 - a_{32} - \gamma) & a_{32} & \gamma & 0 \\ 1 & (1 - b_2 - b_3 - \gamma) & b_2 & b_3 & \gamma \\ \hline & (1 - b_2 - b_3 - \gamma) & b_2 & b_3 & \gamma \end{array}$$

$$a_{32} = \frac{c_3(c_3 - 2\gamma)}{4\gamma} \quad b_2 = \frac{-2 + 3c_3 + 6\gamma(1 - c_3)}{12\gamma(c_3 - 2\gamma)} \quad b_3 = \frac{1 - 6\gamma + 6\gamma^2}{3c_3(c_3 - 2\gamma)} \quad c_3 = \frac{3 - 20\gamma + 24\gamma^2}{4 - 24\gamma + 24\gamma^2}$$

RK334

$$\begin{array}{c|ccc} 0 & 0 & 0 & 0 \\ 2\gamma & \gamma & \gamma & 0 \\ 1 & (1 - b_2 - \gamma) & b_2 & \gamma \\ \hline & (1 - b_2 - \gamma) & b_2 & \gamma \end{array}$$

$$b_2 = (1 - 2\gamma)/(4\gamma) \text{ and } \gamma = (3 + \sqrt{3})/6.$$

Higher-order temporal schemes

Taylor-Green vortex simulation

Analytic solution

$$-\pi \le x, y \le \pi$$

$$u = -\sin(x)\cos(y)e^{-2\nu t}$$

$$v = \cos(x)\sin(y)e^{-2\nu t}$$

$$p = \frac{\rho}{4}\left[\cos(2x) + \cos(2y)\right]e^{-4\nu t}$$

$$w = -2\sin(x)\sin(y)e^{-2\nu t}$$ vortisity

Computational conditions

$$\mathrm{Re} = \frac{U_{\max} L}{\nu} = 10 \qquad L = 2\pi \qquad U_{\max} = 1$$

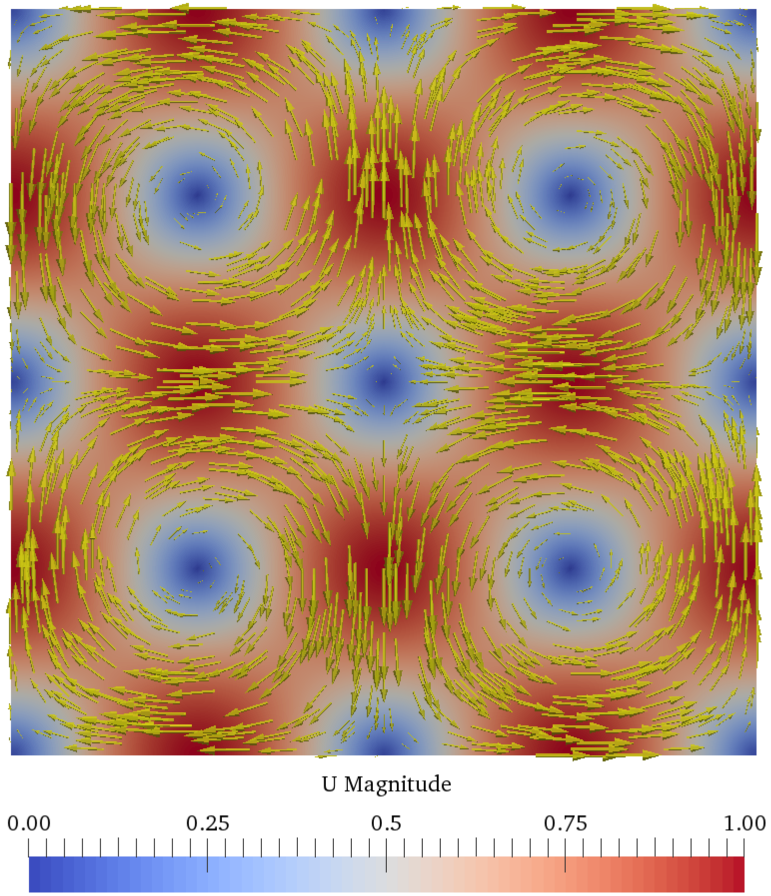

VelocityMag + VelocityVector

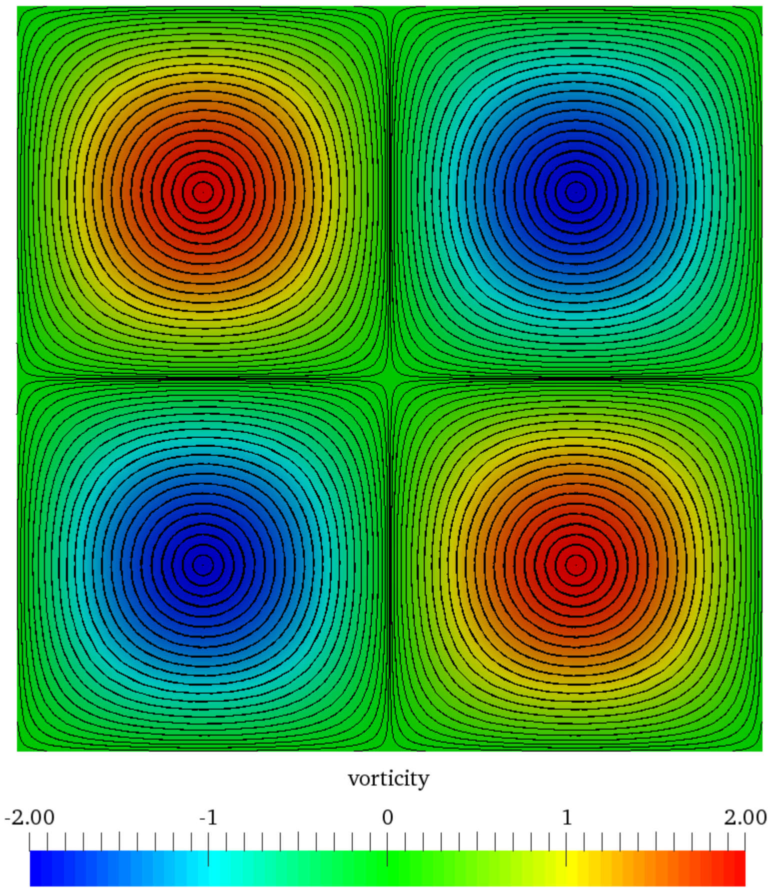

Vortisity + Streamline

Higher-order temporal schemes

Taylor-Green vortex simulation

$t_{end} = 2\,\mathrm{sec}$

maximum error of velocity magintude

maximum error of pressure

Spatial Convergence of velocity

All spatial schemes are linear

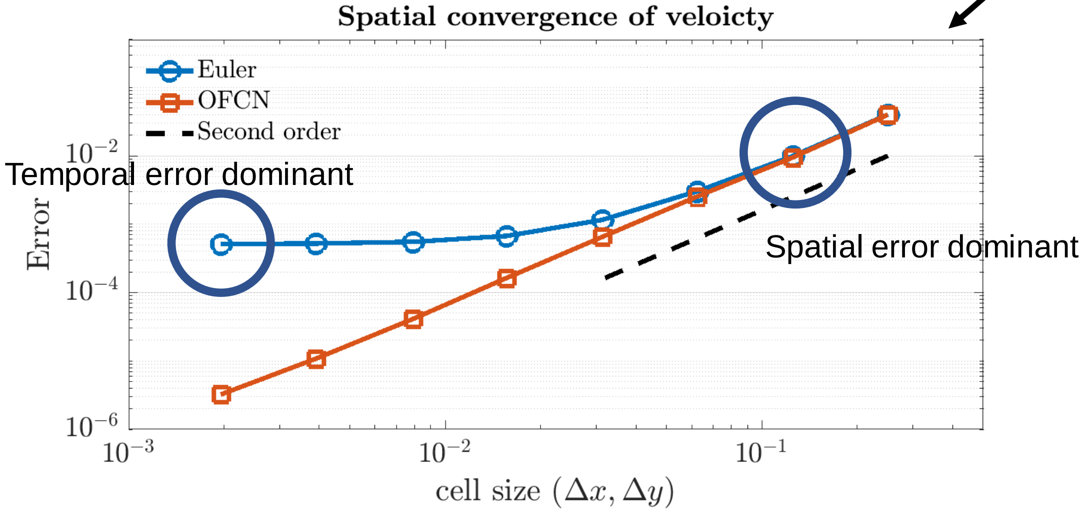

Table 3

The computational conditions of Taylor-Green vortex benchmark, $Re = 10$

Time-step	Number of cell per reference length L			
	Dx04 ∼ Dx64	Dx128	Dx256	Dx512
0.004	O	O	O	O
0.01		O	O	
0.02		O	O	
0.04		O	O	
0.08		O	O	
0.1		O	O	
0.125		O	O	
0.2		O	O	
0.25		O	O	
0.4		O	O	

Spatial

Temporal

Higher-order temporal schemes

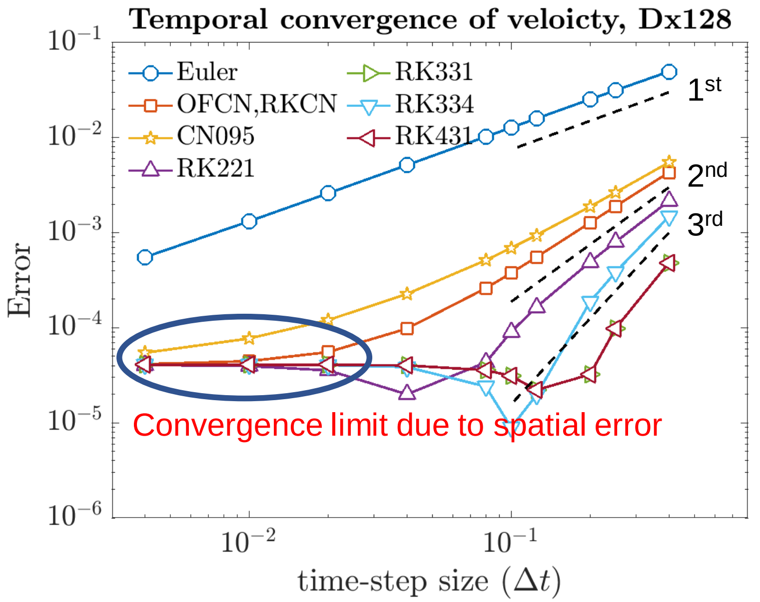

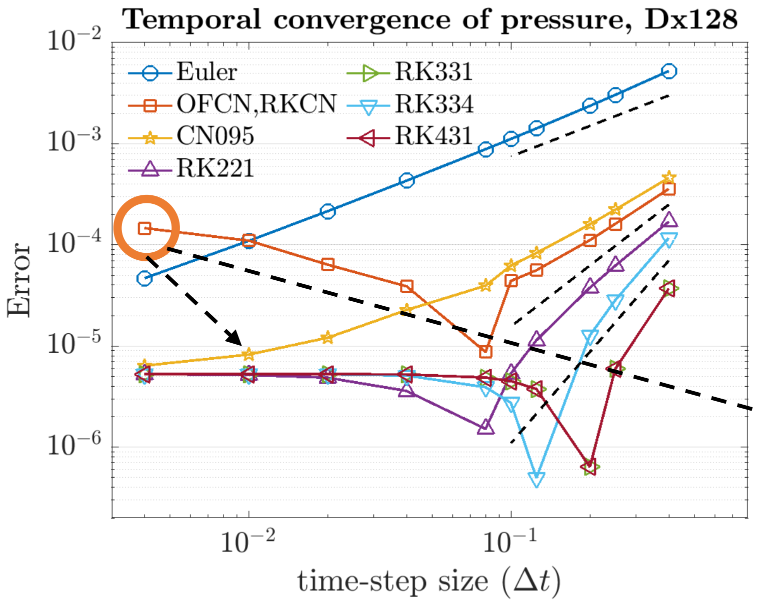

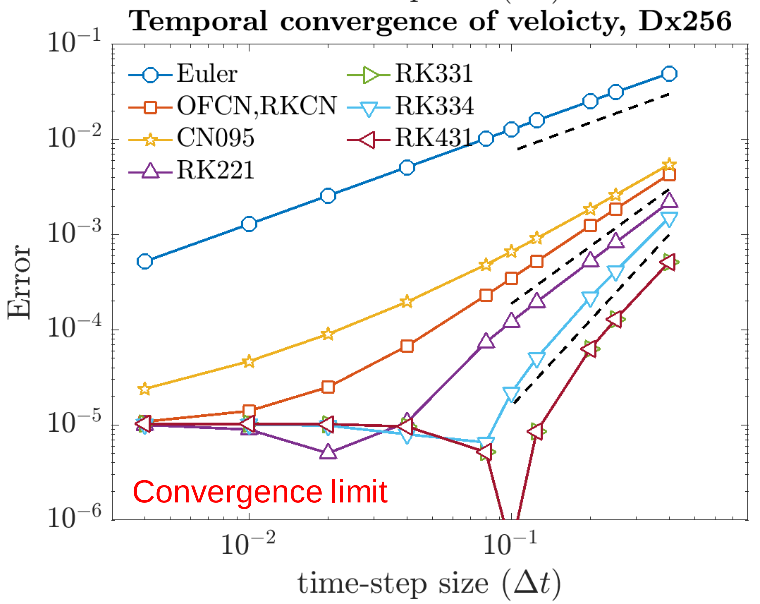

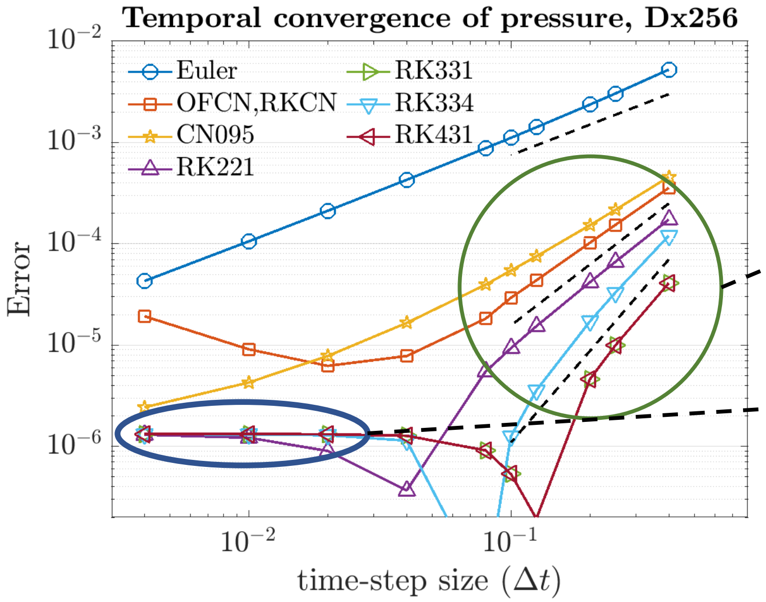

Table 3
The computational conditions of Taylor-Green vortex benchmark, $Re = 10$

Time-step	Number of cell per reference length L			
	Dx04 ∼ Dx64	Dx128	Dx256	Dx512
0.004	O	O	O	O
0.01		O	O	
0.02		O	O	
0.04		O	O	
0.08		O	O	
0.1		O	O	
0.125		O	O	
0.2		O	O	
0.25		O	O	
0.4		O	O	

Spatial

Temporal

Unstable pressure

This can be remedied using off-centering

$$\frac{y^{(n+1)} - y^{(n)}}{h} = C_{CN} f(t^{(n+1)}, y(t^{(n+1)})) + (1 - C_{CN}) f(t^{(n)}, y(t^{(n)})) \quad (37)$$

$$C_{CN} = 1/(1 + C_{oc})$$

Temporal error dominant condition

The order of convergence is achieved.

Spatial error dominant condition

Higher-order temporal schemes

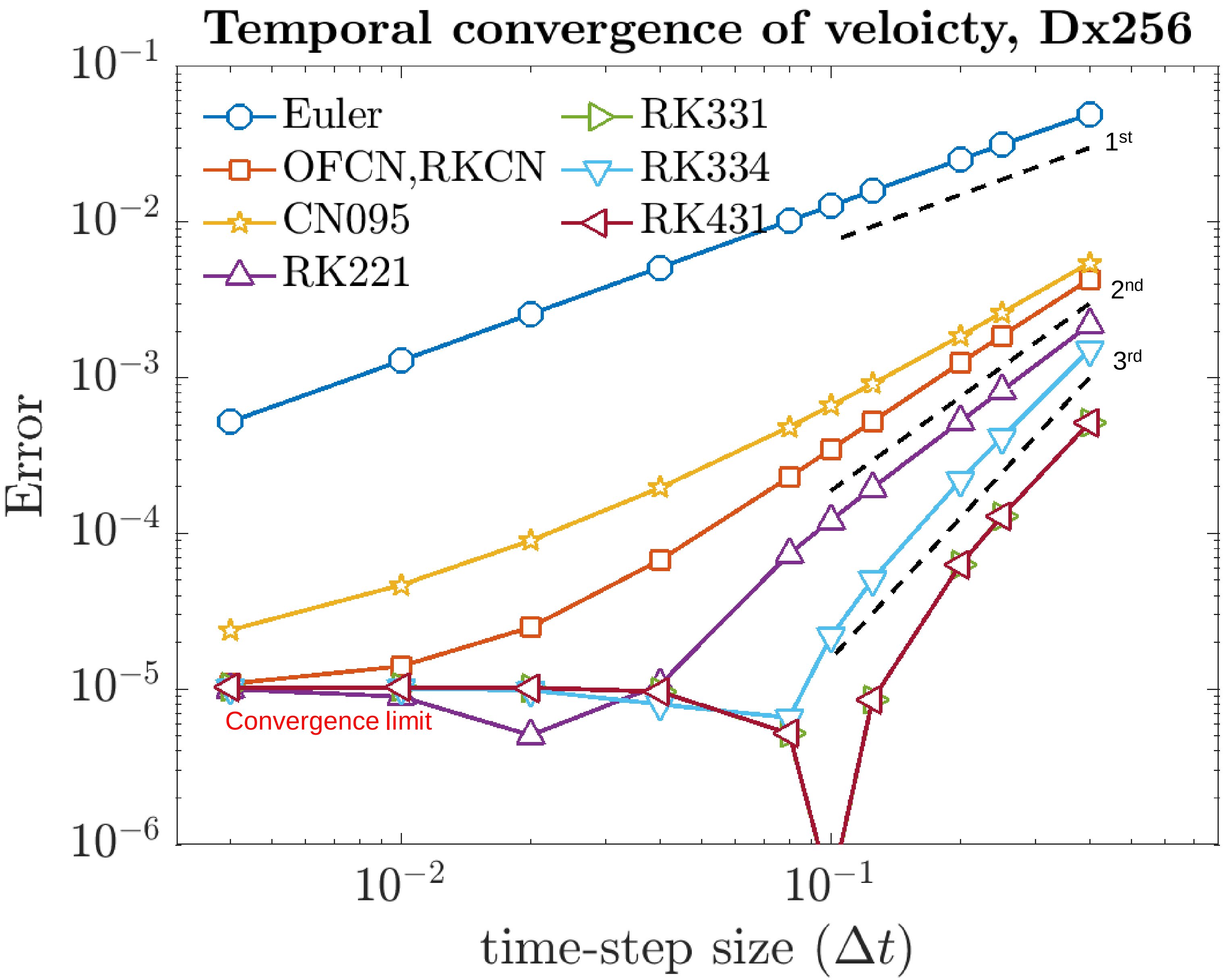

Table 3
The computational conditions of Taylor-Green vortex benchmark, $Re = 10$

Time-step	Number of cell per reference length L			
	Dx04 ~ Dx64	Dx128	Dx256	Dx512
0.004	O	O	O	O
0.01		O	O	
0.02		O	O	
0.04		O	O	
0.08		O	O	
0.1		O	O	
0.125		O	O	
0.2		O	O	
0.25		O	O	
0.4		O	O	

Spatial

Temporal

Higher-order temporal schemes

Periodic wave propagation

Case	$\lambda/\Delta x$	$H/\Delta z$	$T/\Delta t$
Grid 1	25	5	100
Grid 2	50	10	200
Reference Grid 3	100	20	400
Grid 4	200	40	800
Grid 3 dt100	100	20	100
Grid 3 dt200	100	20	200
Grid 3 dt400	100	20	400
Grid 3 dt800	100	20	800
Grid 3 dt1600	100	20	1600

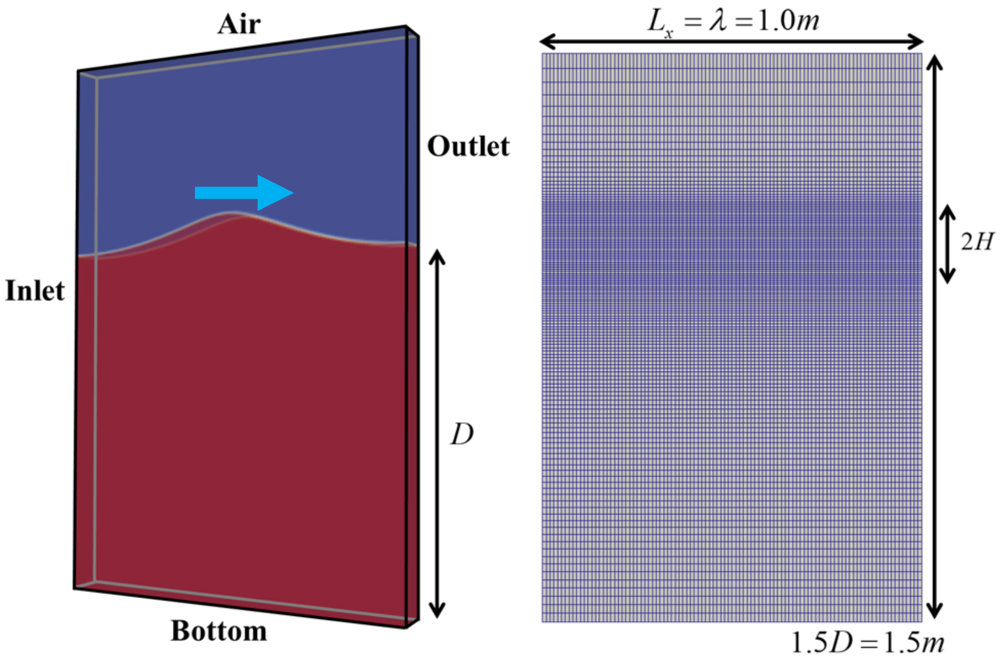

$$\text{Efficiency} = \frac{Accuracy}{Computational\ cost} \rightarrow \frac{\text{Averaged normalized wave amplitude from 1-10 periods}}{\text{(Computation time) x (nCore)}}$$

Higher-order temporal schemes

Periodic wave propagation

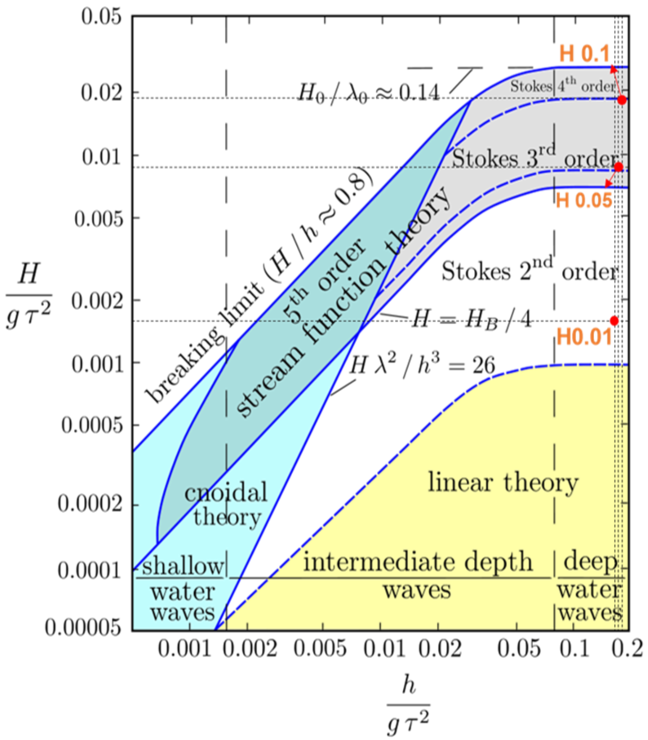

Item	Unit	H0.1	H0.05	H0.01
Depth (D)	[m]	1.0	1.0	1.0
Wave length	[m]	1.0	1.0	1.0
Wave period (T)	[sec]	0.76179	0.79049	0.79991
Wave height (H)	[m]	0.1	0.05	0.01
Wave steepness	H/L	10%	5%	1%
1st order Amp	[m]	0.047413	0.024751	0.004998
2nd order Amp	[m]	0.008294	0.001995	0.000079
3rd order Amp	[m]	0.002263	0.000243	0.000002
4th order Amp	[m]	0.000744	0.000035	-

$$\text{Efficiency} = \frac{Accuracy}{Computational\ cost} \rightarrow \frac{\text{Averaged normalized wave amplitude from 1-10 periods}}{\text{(Computation time) x (nCore)}}$$

Higher-order temporal schemes

Case	$\lambda/\Delta x$	$H/\Delta z$	$T/\Delta t$
Grid 1	25	5	100
Grid 2	50	10	200
Grid 3	100	20	400
Grid 4	200	40	800
Grid 3 dt100	100	20	100
Grid 3 dt200	100	20	200
Grid 3 dt400	100	20	400
Grid 3 dt800	100	20	800
Grid 3 dt1600	100	20	1600

Periodic wave propagation

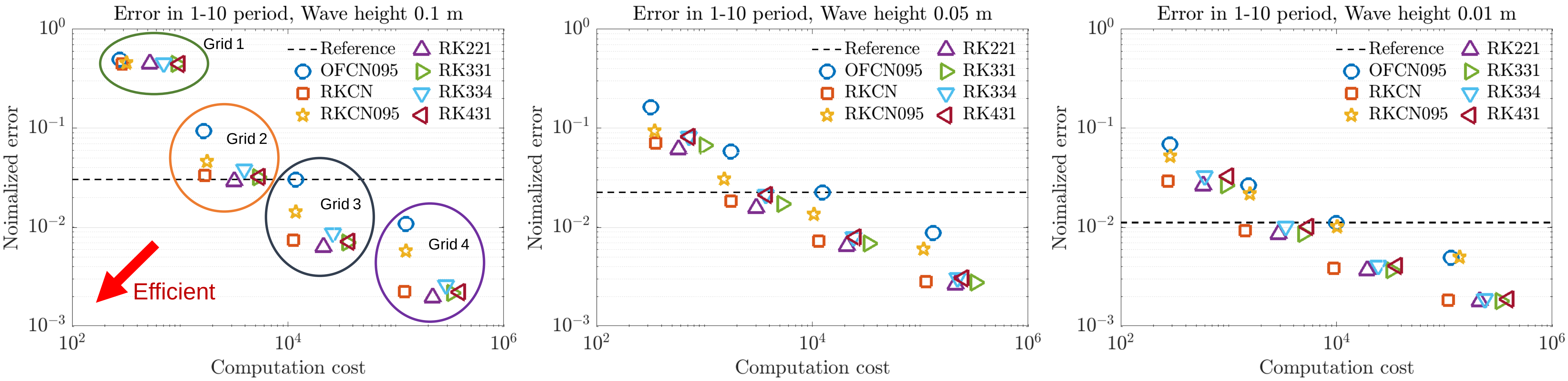

Height 0.1 Height 0.05 Height 0.01

Black dotted line is reference OFCN095 case

Only spatial convergence cases are plotted here to estimate the spatial error.

Higher-order temporal schemes

Case	$\lambda/\Delta x$	$H/\Delta z$	$T/\Delta t$
Grid 1	25	5	100
Grid 2	50	10	200
Grid 3	100	20	400
Grid 4	200	40	800
Grid 3 dt100	100	20	100
Grid 3 dt200	100	20	200
Grid 3 dt400	100	20	400
Grid 3 dt800	100	20	800
Grid 3 dt1600	100	20	1600

Periodic wave propagation

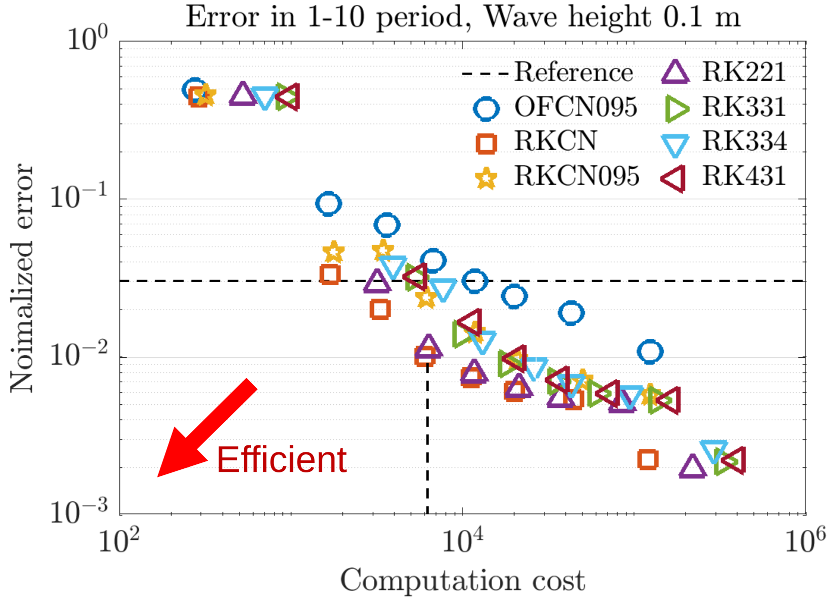

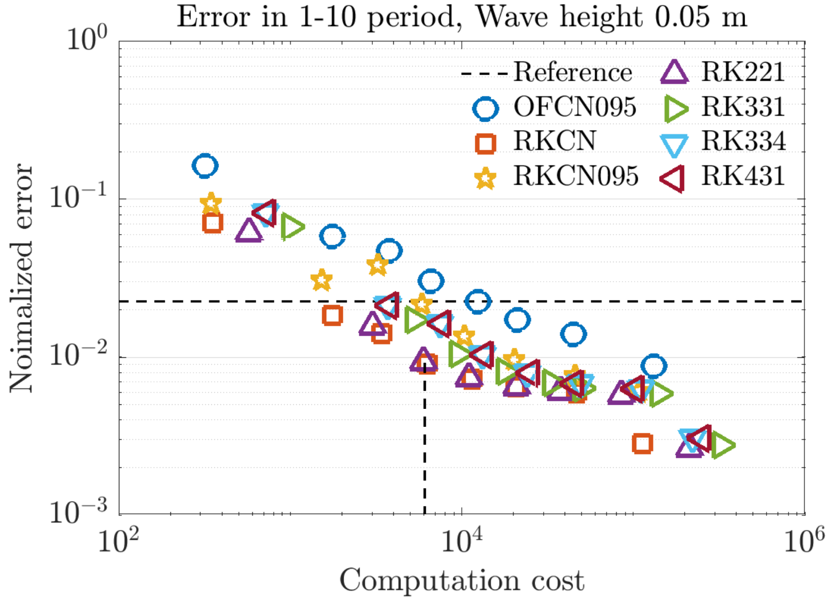

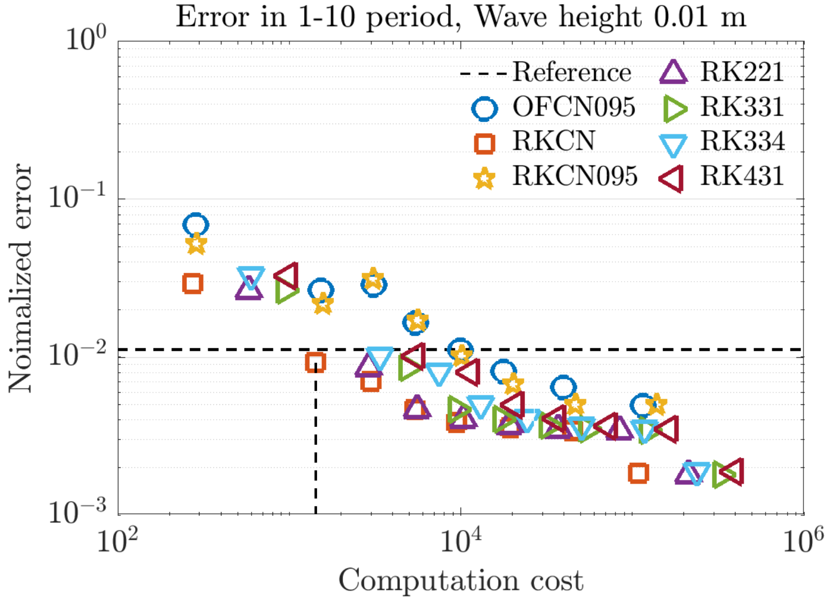

The efficient solvers are RKCN and RK221

Higher-order rate of convergences are not observed.

Better stability is observed with SDIRK_SA type methods

If the wave amplitudes are small, we can use courser mesh

Code name	Identification name	Order	Implicit stage
Euler	Implicit Euler	1	1
OFCN	OpenFOAM CN	2	1
RKCN	ESDIRK[2](2)_SA	2	1
RK221	SDIRK[2](2)_S	2	2
RK331	SDIRK[3](3)_SA	3	3
RK334	ESDIRK[3](3)_SA	3	2
RK431	ESDIRK[3](4)_SA	3	3

Higher-order temporal schemes

Case	$\lambda/\Delta x$	$H/\Delta z$	$T/\Delta t$
Grid 1	25	5	100
Grid 2	50	10	200
Grid 3	100	20	400
Grid 4	200	40	800
Grid 3 dt100	100	20	100
Grid 3 dt200	100	20	200
Grid 3 dt400	100	20	400
Grid 3 dt800	100	20	800
Grid 3 dt1600	100	20	1600

Periodic wave propagation with moving mesh

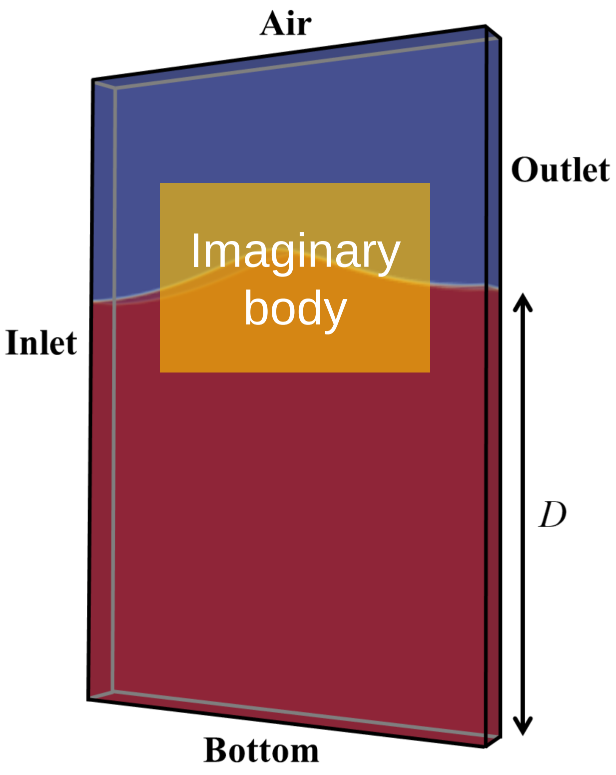

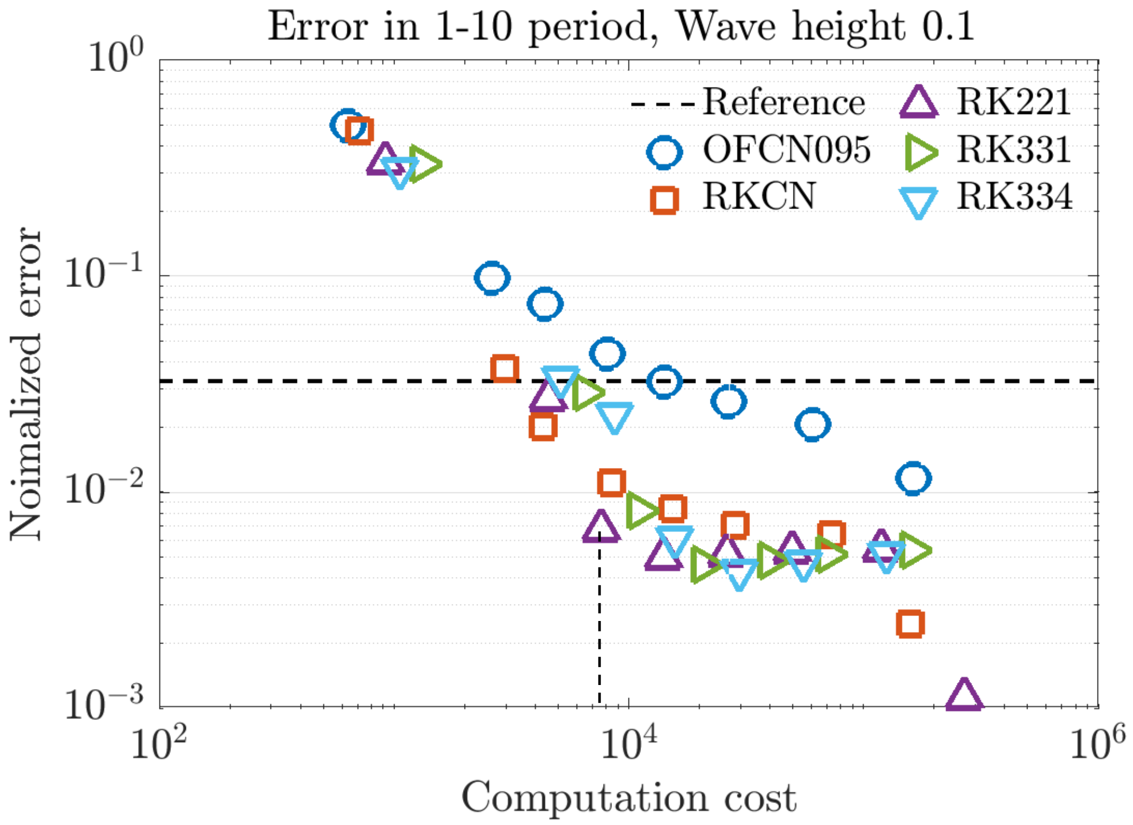

Error increased compare to the static mesh cases

DIRK type methods are more efficient then classical OFCN

Higher-order temporal schemes

Future works

To do a FSI simulation it is good to use SWENSE to control the number of cell.

$$\chi = \chi_I + \chi_C$$

= incident wave component + complimentary component

1. CALM buoy in regular / irregular wave

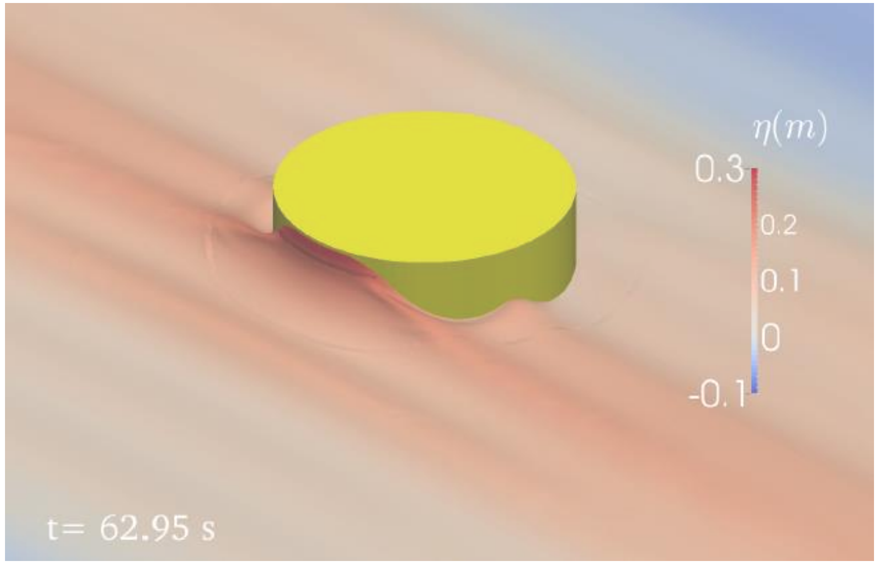

2. KCS with waves & with forward speed

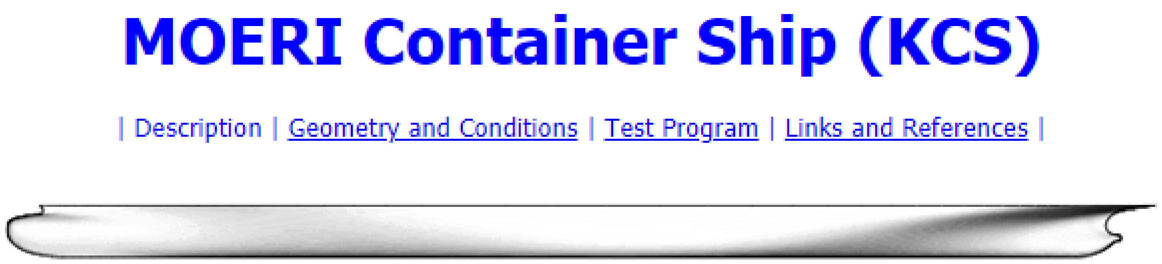

Higher-order spatial schemes

Future works

WENO & WENO reconstruction method.

$$p_{WENO,i} = \bar{\Phi}_i + \sum_{k=1}^{K} \tilde{a}_k \Omega_k \quad \longleftarrow \quad p_{weno} = \sum_{m=1}^{N_{si}} w_m p_i^{(m)} \quad \longleftarrow \quad p_i^{(m)} = \bar{\Phi}_i + \sum_{k=1}^{K} a_k^{(m)} \Omega_k$$

N_{si}=stencils

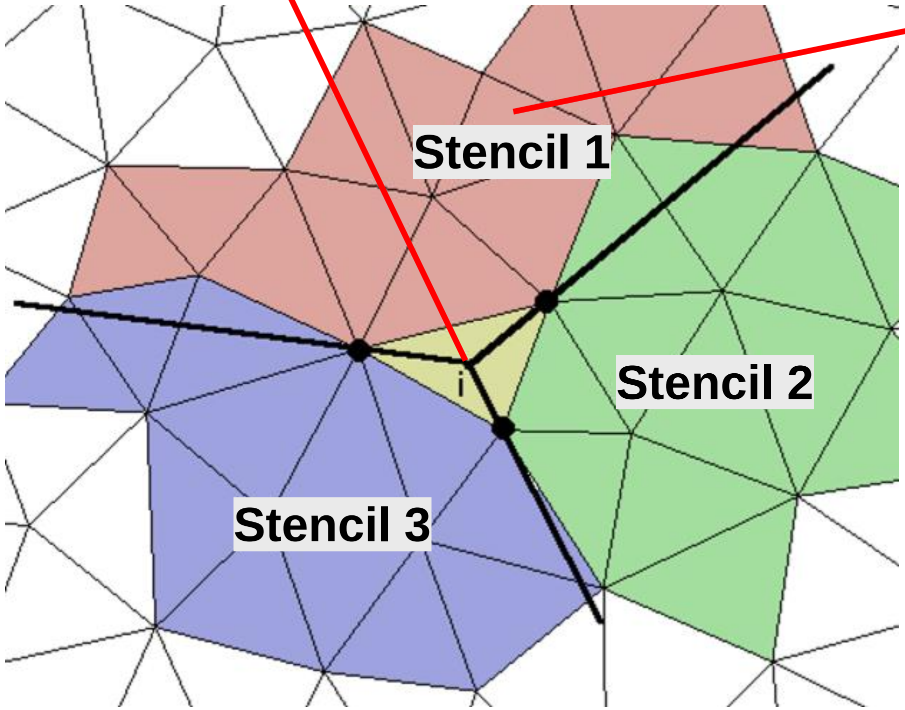

Need careful formulation
also needs to estimate its efficiency.

Articles

1. A paper on the higher-order temporal scheme (ongoing).
2. A paper on the interface treatment schemes (Not ready yet).

Higher-order temporal schemes

Solve α Equation

Predictor:
Solve intermediate VOF with upwind(bounded) flux

Set Bounded flux

Corrector:
Correct VOF with MULES

MULES loop

Updates for MULES iteration

Update VOF & Mass flux

$i = 1:s$ Runge-Kutta iiteration label

$$\frac{V_P^{(i)}\alpha_P^{*(i)} - V_P^{(n)}\alpha_P^{(n)}}{h} + a_{ii}\sum_{faces}\left(\phi_f\alpha^*\right)^{(i)}_{BD} + \boxed{\sum_{j}^{s-1} a_{ij}\sum_{faces}\left(\phi_f\alpha\right)^{(j)}_{BD}}$$

$$\begin{array}{c|cccc} \tau_1 & a_{11} & 0 & 0 & 0 \\ \tau_2 & a_{21} & a_{22} & 0 & 0 \\ \tau_3 & a_{31} & a_{32} & a_{33} & 0 \\ \tau_4 & a_{41} & a_{42} & a_{43} & a_{44} \\ \hline & b_1 & b_2 & b_3 & b_4 \end{array}$$

$$F_{BD}^{(i)} = \sum_{faces}\left[\left(\phi_f\alpha^*\right)^{(i)}_{BD}\right]$$

$$\frac{V_P^{(i)}\alpha_P^{**(i)} - V_P^{(i)}\alpha_P^{*(i)}}{h} + \lambda\left[a_{ii}\sum_{faces}F_{Corr}\left(\phi_f\alpha^*\right)^{(i)} + \sum_{j}^{s-1} a_{ij}\sum_{faces}F_{Corr}\left(\phi_f\alpha\right)^{(j)}\right]$$

$$F_{Corr}\left(\phi_f\alpha^*\right)^{(i)} = \sum_{faces}\left[\left(\phi_f\alpha^*\right)^{(i)}_{UB} + \left(\phi_{r,f}\alpha^*\left(1-\alpha^*\right)\right)^{(i)}_{UB}\right] - F_{BD}^{(i)}$$

$$F_{BD}^{(i)} = \sum_{faces}\left[\left(\phi_f\alpha^*\right)^{(i)}_{BD}\right] + \lambda\left[\sum_{faces}\left[\left(\phi_f\alpha^*\right)^{(i)}_{UB} + \left(\phi_{r,f}\alpha^*\left(1-\alpha^*\right)\right)^{(i)}_{UB}\right]\right]$$

$\alpha^* = \alpha^{**}$ Update intermidiate VOF for MULES iteration

$$\alpha^{(i)} = \alpha^{**} \qquad \left(\rho\phi\right)^{(i)} = F_{BD}^{(i)}\left(\rho_{water} - \rho_{air}\right) + \phi^{(i)}\rho_{air}$$

Higher-order temporal schemes

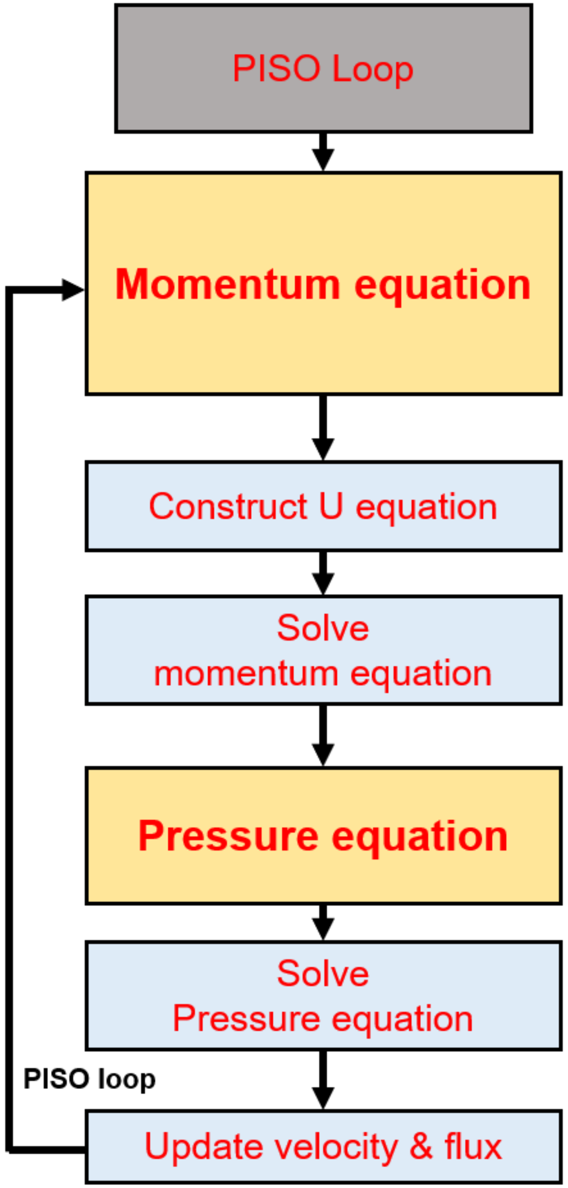

$$\frac{\partial(V_P\rho\boldsymbol{u})}{\partial t}+\sum_{faces}\left((\rho\phi)_f\,\boldsymbol{u}_f\right)-\sum_{faces}\left(\mu_f\left(\nabla\boldsymbol{u}_f\right)\right)-\nabla\boldsymbol{u}\cdot\nabla\mu V_P=\nabla p_d V_P-(\boldsymbol{g}\cdot\boldsymbol{x})\nabla\rho V_P$$

$$RKi=i=1:s$$

$$\frac{(V_P\rho\boldsymbol{u})^{(i)}-(V_P\rho\boldsymbol{u})^{(n)}}{h}+a_{ii}\boldsymbol{R}^{(i)}+\boxed{\sum_{j=1}^{i-1}a_{ij}\boldsymbol{R}^{(j)}}=0$$

$$\begin{array}{c|cccc}
\tau_1 & a_{11} & 0 & 0 & 0\\
\tau_2 & a_{21} & a_{22} & 0 & 0\\
\tau_3 & a_{31} & a_{32} & a_{33} & 0\\
\tau_4 & a_{41} & a_{42} & a_{43} & a_{44}\\
\hline
 & b_1 & b_2 & b_3 & b_4
\end{array}$$

$$\boldsymbol{R}^{(i)}=\sum_{faces}\left((\rho\phi)_f^{(i)}\,\boldsymbol{u}_f^{(i)}\right)-\sum_{faces}\left(\mu_f^{(i)}\left(\nabla\boldsymbol{u}_f^{(i)}\right)\right)-\nabla\boldsymbol{u}^{(i)}\cdot\nabla\mu^{(i)}V_P^{(i)}+\nabla p_d^{(i)}V_P^{(i)}+(\boldsymbol{g}\cdot\boldsymbol{x})\nabla\rho^{(i)}V_P^{(i)}$$

$$UEq^{(i)}=\boldsymbol{a}_P^{(i)}\boldsymbol{u}^{(i)}-\boldsymbol{H}^{(i)}=-a_{ii}\nabla p_d^{(i)}-a_{ii}\nabla\rho^{(i)}(\boldsymbol{g}\cdot\boldsymbol{x})^{(i)}$$

Get $\boldsymbol{u}^{(i)}$

$$\nabla\boldsymbol{u}^{(i)}=0=\nabla\frac{1}{\boldsymbol{a}_P^{(i)}}\left[\boldsymbol{H}^{(i)}-a_{ii}\nabla p_d^{(i)}-a_{ii}\nabla\rho^{(i)}(\boldsymbol{g}\cdot\boldsymbol{x})^{(i)}\right]$$

$$\sum_{faces}\left[\frac{1}{\boldsymbol{a}_P^{(i)}}a_{ii}\nabla p_d^{(i)}\right]_f=\sum_{faces}\left(\frac{1}{\boldsymbol{a}_P^{(i)}}\left[\boldsymbol{H}^{(i)}-a_{ii}\nabla\rho^{(i)}(\boldsymbol{g}\cdot\boldsymbol{x})^{(i)}\right]\right)_f$$

$$\boldsymbol{u}^{(i)}=\frac{1}{\boldsymbol{a}_P^{(i)}}\left[\boldsymbol{H}^{(i)}-a_{ii}\nabla p_d^{(i)}-a_{ii}\nabla\rho^{(i)}(\boldsymbol{g}\cdot\boldsymbol{x})^{(i)}\right]$$

Higher-order temporal schemes: ALE

3.4.1. Application of ALE formulation

The consideration of moving mesh to VOF convection equation write: The additional term, mesh flux (ϕ_{mesh}), is also adapted to *Predictor & Corrector* algorithm.

$$\frac{V^{(i)}_{P(n+1)}\alpha^{(i)}_{P(n+1)} - V^{(n)}_{P(n+1)}\alpha^{(n)}_{P(n+1)}}{h} + \underline{\sum_f (\phi_{mesh}\alpha_f)^{(i)}} + a_{ii}\sum_f (\phi_f\alpha_f)^{(i)} + \sum_{j=1}^{i-1} a_{ij}\sum_f (\phi_f\alpha_f)^{(j)} = 0. \tag{32}$$

The application of SCL formulation to momentum equation yields Eq.($\boxed{33}$), where the **R** is equal to Eq.($\boxed{24}$).

$$\frac{(V\rho\mathbf{u})^{(i)}_P - (V\rho\mathbf{u})^{(n)}_P}{h} + \underline{\sum_f \left[(\rho\phi_{mesh})^{(i)}\mathbf{u}^{(i)}_f\right]} + a_{ii}\mathbf{R}^{(i)} + \sum_{j=1}^{i-1} a_{ij}\mathbf{R}^{(j)} \tag{33}$$

Preliminary study: Waves

Wave generation and absorption.

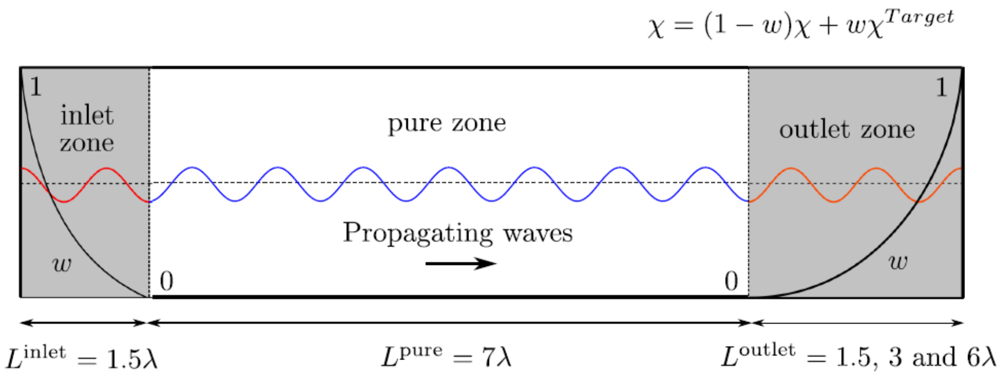

Figure 1.1. Schematic view of the NWT for a parametric study on the relaxation schemes.

Explicit Relaxation method (to incident wave & no wave).

Increased viscosity & artificial damping source

$$\frac{\partial(\rho \boldsymbol{u})}{\partial t} + \nabla\cdot(\rho \boldsymbol{u}\boldsymbol{u}) - \nabla\cdot\left((\mu + \mu_{add})(\nabla \boldsymbol{u})\right) - \nabla \boldsymbol{u}\cdot\nabla\mu = \nabla p_d - (\boldsymbol{g}\cdot\boldsymbol{x})\nabla\rho + \boldsymbol{S}$$

$$\boldsymbol{S} = \left(0, 0, \rho\left(C_1 + C_2 u_z\right) w u_z\right)$$

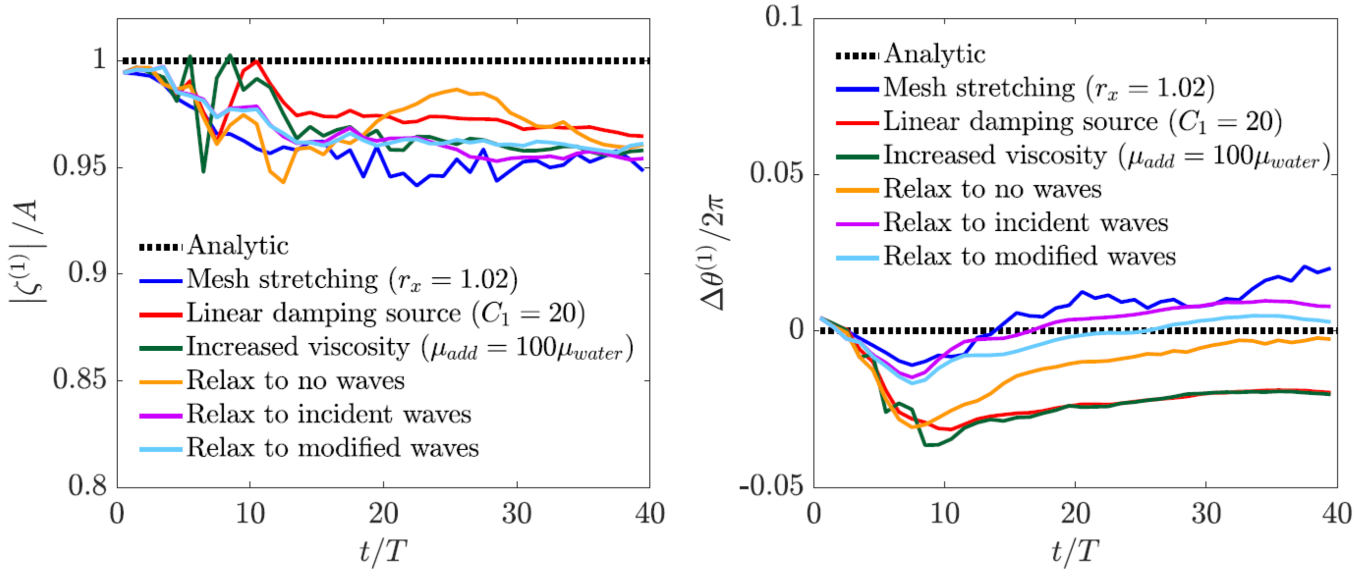

(a) Amplitude **(b)** Phase differences

Figure 2.1. The first-order harmonic amplitudes and phase differences with respect to different outlet.

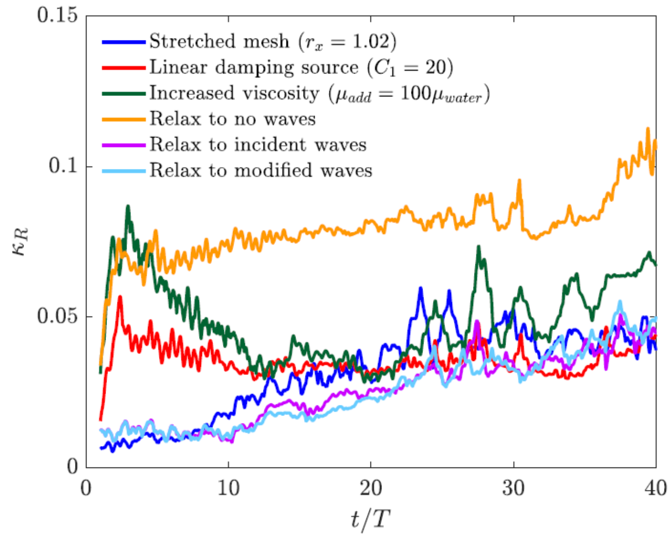

Figure 2.2. Evolution of reflection coefficients for different outlets.